Asian Journal of Chemistry; Vol. 31, No. 8 (2019), 1809-1814

ASIAN JOURNAL OF CHEMISTRY

https://doi.org/10.14233/ajchem.2019.22024

Green Synthesis and Characterization of α-Fe_2O_3 Nanoparticles using Leaf Extract of *Syzygium cumini* and their Suitability for Adsorption of Cu(II) and Pb(II) Ions

NAVEEN CHANDRA JOSHI*, AKSHITA CHODHARY, YASHWINI PRAKASH and AJAY SINGH

Department of Chemistry, Uttaranchal University, Dehradun-248007, India

*Corresponding author: E-mail: drnaveen06joshi@gmail.com

Received: 23 February 2019; *Accepted*: 13 April 2019; *Published online*: 28 June 2019; AJC-19457

In the present study, we have synthesized α-Fe_2O_3 nanoparticles by using the leaf extract of *Syzygium cumini*. The applying green synthetic process is very efficient, low cost and can be applicable in the large scale operations. The freshly synthesized dried nanoparticles were characterized by UV-visible, FT-IR, XRD and FESEM. The α-Fe_2O_3 (haematite) nanoparticles have now used as effective nano-adsorbents for the removal of Cu(II) and Pb(II) ions from synthetically prepared wastewater under batch conditions. The batch system included contact time, dosage, pH, concentration and temperature. The maximum adsorption efficiency was found at optimized conditions such as contact time 60 min, higher acidic pH 6, higher dosage of sorbent 1.0 g and lower metal ion concentration 10 mg/L. For Pb(II) ions, 59.79, 85.10, 51.39 and 36.81 % adsorption was found at contact time 60 minutes, pH 6, dosage 1 g and metal ion concentration 10 mg/L. Similarly, for Cu(II) ions at same conditions, the adsorption was found to be 49.88, 69.73, 53.77 and 20.68 %, respectively. The equilibrium data of adsorption have been tested by Langmuir, Freundlich and Temkin isotherm models. The adsorption data were best fitted to Langmuir isotherm model with the regression values R^2 = 0.984 for Cu(II) ions and R^2 = 0.9383 for Pb(II) ions. The adsorption capacity of α-Fe_2O_3 nanoparticles for Cu(II) and Pb(II) ions was found 7.535 and 6.480 mg/g, respectively.

Keywords: Green synthesis, Nano-adsorbents, Characterizations, Adsorption, Isotherm models.

INTRODUCTION

Green synthetic approaches in the fields of chemistry are the better alternatives over conventional synthetic processes. These newly approaches are efficient, simple, low cost, environmentally friendly and can be applicable in large scale manufacturing processes [1]. The adsorption based removal of heavy metal ions from wastewater is a good alternative over the conventional methods like precipitation, electro-winning, reverse osmosis, pre-concentrations, ultrafiltration and ion exchange [2,3]. In environmental chemistry, metal oxide nanoparticles play an important role for the adsorption based removal of heavy metals from the waters or wastewaters [4]. Various types of adsorbents are reported in the literature such as carbon nanotubes, activated carbon, polymeric adsorbents, metal oxides and biosorbents [5-18]. Among these iron based nanomaterials show unique properties like larger surface area/volume ratio, good adsorption capacities for contaminants and no harmful sludge generation [1]. Iron oxides are found in three forms *i.e.* magnetite (Fe_3O_4), hematite (α-Fe_2O_3) and maghemite (α-Fe_2O_3). The hematite form is very common and better than other forms in the recovery point of view of the adsorbents [19,20]. Heavy metals have high relative densities and atomic weights, some of them are necessary for the vital activities in living organisms under the concerned limits but many of them are very harmful even at very low concentrations [21].

Copper is released in the environment due to aerosol, rock weathering, fossil fuel burning and nuclear power plants. Copper is an essential element and helps in the iron utilization and blood formation. The excess side effects of copper are lever damage, gastrointestinal catarrah and chronic poisoning [16]. Lead is the most common heavy metal that releases in the environment through battery recycling, smelting, leaded gasoline, lead containing pipes etc. It is very harmful to reproductive, urinary and nervous system and a carcinogenic agent; in plants, lead retards the rate of photosynthesis [2]. In the present investigations, haematite nanoparticles have been synthesized by using the leaf extract of waste leaves of *Syzygium cumini*. This

plant is commonly known as black palm or jamun or jambolan and sometimes blackberry. The leaves of *Syzygium cumini* are leathery, obovate-elliptic, smooth and 7-11 cm long. These leaves contained acylated flavonol glycosides, tannin, triterpenoids, esterase, galloyl carboxylase, myricitin, quercetin, *etc*. [22].

EXPERIMENTAL

Green synthesis of α-Fe_2O_3 nanoparticles: The collected leaves of *Syzygium cumini* were washed 2-3 times with double distilled water and cut into small pieces. The 30 g cut leaves boiled for 30 min with 200 mL of double distilled water in a 500 mL Erlenmeyer flask at 80 ºC for 1 h on a magnetic stirrer hot plate. After boiling, filter the content and filtrate *i.e*. leaf extract was preserved at 4 ºC for further studies. Anhydrous ferric chloride of Analytical grade was used as initial precursor and a requisite amount of ferric chloride was added in deionized water. After that, 10 mL of extract is added in 100 mL of $FeCl_3$ solution; the colour of solution changed from brownish to blue-violet colour. The reaction mixture was then centrifuged at 10,000 rpm for 15 min and the nanoparticles were allowed to settled down. The obtained nanoparticles washed with double distilled water and dried at 250 ºC under controlled conditions. Finally, well-defined nanoparticles of iron oxide were collected and preserved for characterizations and adsorption studies.

Preparation of synthetic wastewater: The synthetic wastewater containing Cu(II) and Pb(II) ions was prepared by dissolving a desired amount of copper acetate and lead acetate in double distilled water. For making 1000 mg/L of stock solutions, 2.858 g of copper acetate dihydrate and 1.569 g of lead acetate were dissolved separately in double distilled water and the pH of this solution was maintained at pH 4 by using digital pH meter. All working solutions of wastewater having concentrations 10-50 mg/L and pH 2-6 were prepared by the dilution of stock solutions. The pH of all solutions was adjusted by using 0.1M HCl or 0.1M NaOH solutions.

Adsorption studies: The adsorption study was carried out under batch system that included contact time (10 to 70 min), pH 2-6, dosage (0.1 to 1 g), concentration (10 to 50 mg/L) and temperature (10 to 70 ºC). A requisite amount of nano adsorbent was treated with a working solution of desired concentrations. This content was shaken at 150 rpm on a rotatory shaker for a particular time. After that, the solution filtered and the metal ion concentrations was determined in the filtrate by using atomic absorption spectroscopy (Thermo-Fisher Scientific Model AA301). The equilibrium data of adsorption have been tested with different isotherm models *i.e*. Langmuir, Freundlich and Temkin isotherm models. The percentage adsorption or removal efficiency of metal ions on the surface of nanopowder is calculated as:

$$\text{Adsorption (\%)} = \frac{C_o - C_e}{C_o} \times 100$$

where, C_o and C_e are the metal ion concentrations in the working solutions of synthetically prepared wastewater.

RESULTS AND DISCUSSION

FT-IR analysis: The spectrum of α-Fe_2O_3 nanoparticles synthesized from the leaf extract of *Syzygium cumini* in the range of 4000-500 cm^{-1} was obtained. The FT-IR analysis gives the stretching vibrations at 3403, 3337, 1631, 1446 and 1072 cm^{-1} (Fig. 1). These strong peaks indicated the presence of -OH, -NH, -C=O, C=C and C-C groups on the surface of iron oxide nanoparticles. The IR band at 667 cm^{-1} is due to Fe-O stretching band of iron oxide.

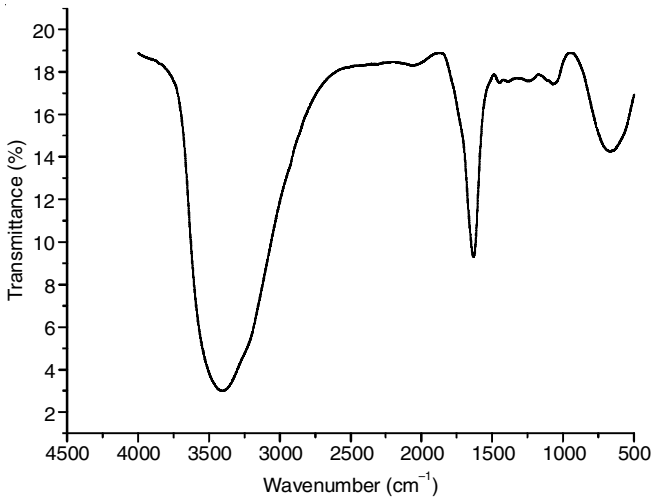

Fig. 1. FT-IR spectra of α-Fe_2O_3 nanoparticles

The formation of iron oxide nanoparticles has also been confirmed by measuring their absorbance with UV-visible spectrophotometer (300-800 nm). The absorption peaks at 360, 397 and 590 nm have been observed for the synthesized α-Fe_2O_3 nanoparticles after 10 min. A strong absorption peak at 590 nm is especially due to excitation of surface plasmon vibrations in the solution of iron oxide nanoparticles (Fig. 2) [23]. Field-emission scanning electron microscope (FESEM) works with electrons instead of light and these electrons are released by a field emission source. The scanning object is scanned by electrons with a zig-zag pattern. Under a high vacuum column the electrons are focussed and deflected by electronic lenses to produce a smooth and narrow beam that bombards the object. FESEM images indicate that the synthesized iron oxide nanoparticles are irregular spherical shaped (Fig. 3).

XRD analysis: The broader peaks (Fig. 4) in the XRD pattern of iron oxide confirmed the formation of α-Fe_2O_3 nano-

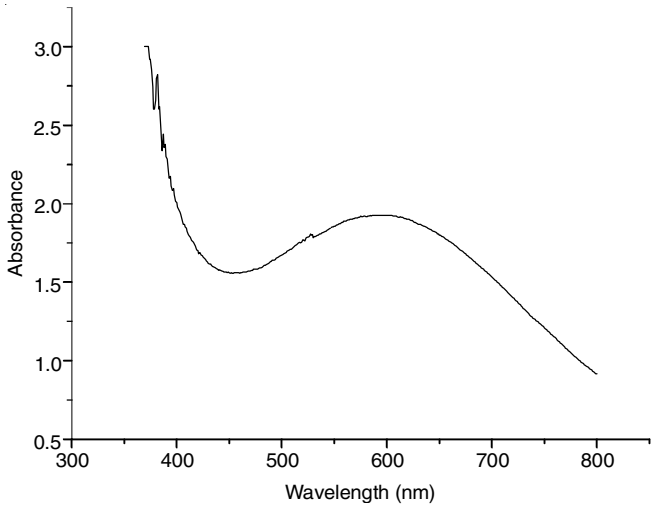

Fig. 2. UV-visible spectra of α-Fe_2O_3 nanoparticles

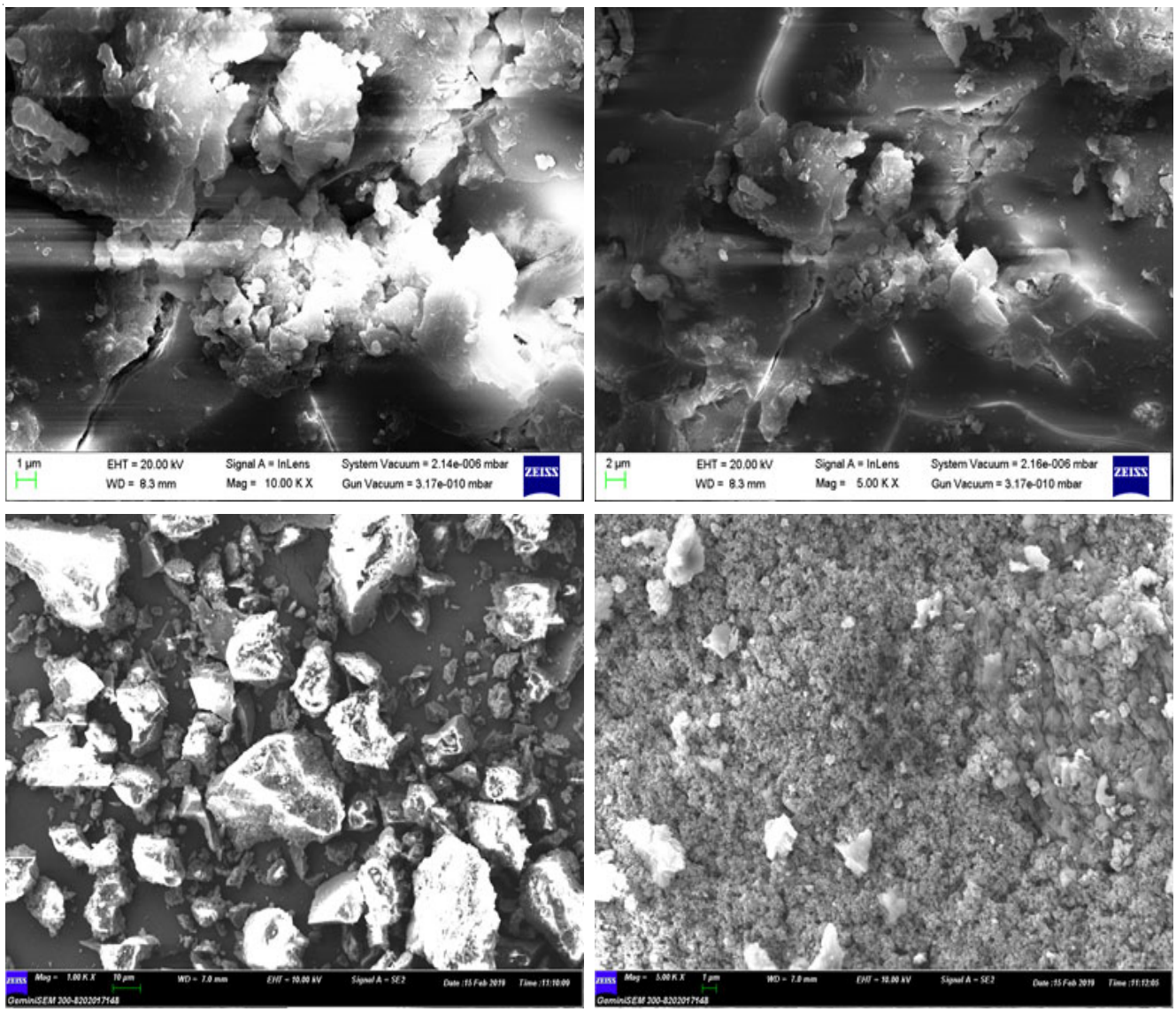

Fig. 3. FESEM images of α-Fe_2O_3 nanoparticles

particles [24]. The characteristic peaks of α-Fe_2O_3 nanoparticles were observed at 23.8º (012), 36.02º (110), 38.73º (320) 49.80º (024), 62.70º (214) and 61.17º (300) in the XRD pattern (Fig. 4).

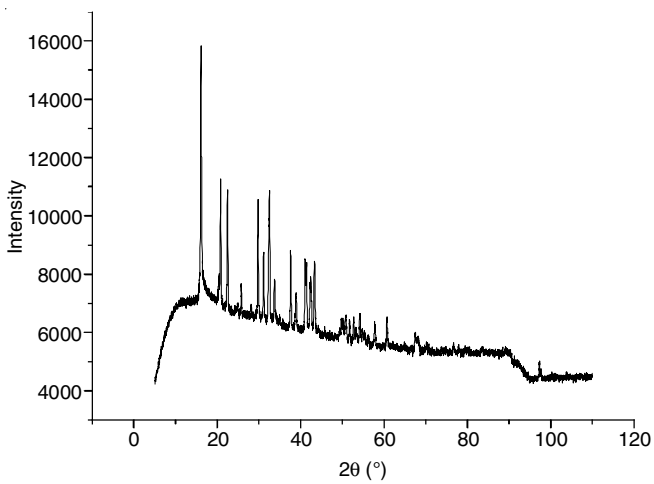

Fig. 4. XRD pattern of α-Fe_2O_3 nanoparticles

Adsorption studies

Effect of dosage and contact time: Initially, the adsorption is found 10.19 and 1.04 % for Cu(II) and Pb(II) ions at 0.1 g of adsorbent. The adsorption increases to 38.41 and 34.69 % for Cu(II) and Pb(II) at 0.5 g of adsorbent dosage (Fig. 5a). The adsorption efficiency increases rapidly with the amount of adsorbent. The maximum adsorption efficiency has been achieved 53.77 and 51.39 % for copper and lead at dosage of 1 g. In general, the adsorptive removal of metal ions increases with the amount of adsorbent due to the increase of number of functional groups with the dosage [25]. A minimum time is required for the interaction of metal ions with active groups. The percentage adsorption increases with contact times due to availability of more active groups that are present on the surface of adsorbent. The adsorption data at different contact or agitation times are very important to determine the rate of adsorption and other kinetic parameters. In the present study, it was found that the adsorption efficiencies 14.18 and 10.79 % for copper(II) and lead(II) ions, respectively and that increases to 39.29 and 54.69 %. The maximum removal was found at

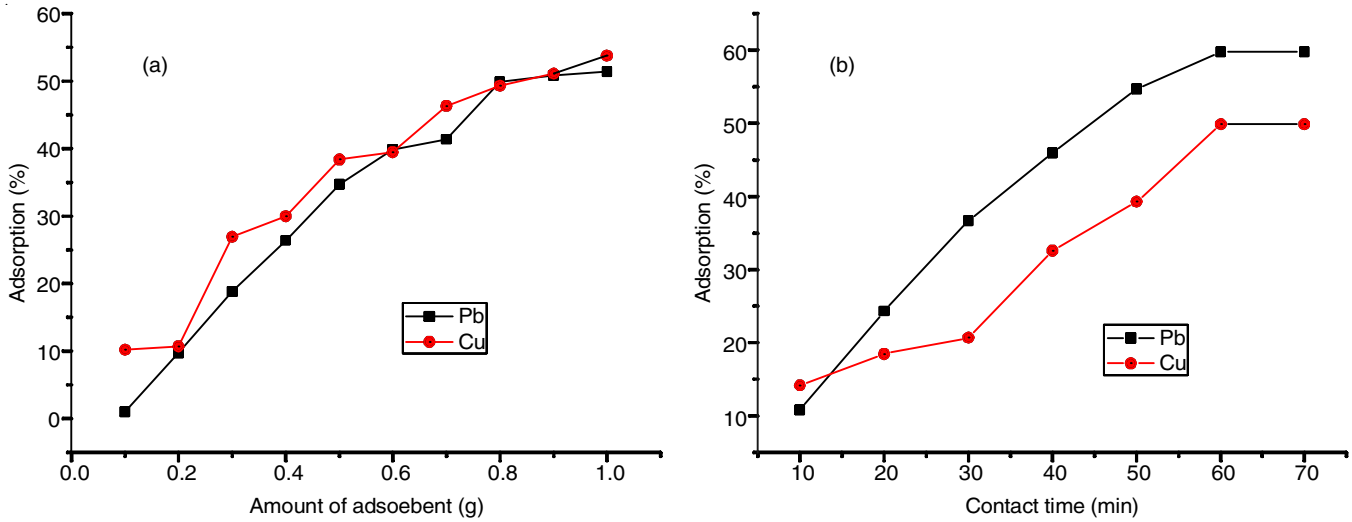

Fig. 5 (a) Effect of dosage (b) Effect of contact time on the removal of copper and lead

contact time 60 min *i.e.* 49.88 and 59.79 % for Cu(II) and Pb(II) ions, respectively. After that the adsorption becomes constant, which may be due to the occupation of all active sites or groups by metal ions [2] (Fig. 5b).

Effect of pH: At lower pH, the adsorption is usually found very low due to protonation of all functional groups present on the surface of adsorbent and so repulsion occurs between metal ions and positively charged functional groups. Maximum adsorption is found at higher acidic pH of solutions because a few active sites become protonated and easily available for interactions with metal ions [12,26]. In present investigations, the adsorption efficiency for copper(II) and lead(II) is found to be 9.65 and 9.9 %, respectively at pH 2, which increases 36.41 and 48.09 % at pH 4. A maximum adsorption was recorded at higher pH 6 *i.e.* 69.73 and 85.10 % for Cu(II) and Pb(II) ions (Fig. 6a).

Effect of temperature: The adsorption of metal ions usually increases with the applied temperature in the batch operations but after a certain temperature it becomes constant or decreases. It is due to the further dissolution of metal ions in the solution from adsorbent at such temperatures [10,11]. The removal of Cu(II) and Pb(II) ions on to nanoparticles increases from 20.97 and 26.39 % at 10 ºC to 36.90 and 49.87 % at 60 ºC; after that the adsorption becomes constant (Fig. 6b).

Effect of concentration: Initially, the removal efficiencies are observed 20.68 and 36.81 % for copper(II) and lead(II), respectively at 10 mg/L. Further, removal efficiencies sharply decrease from the concentration 10 mg/L to 50 mg/L. At 50 mg/L, the percentage adsorptions are observed 9.97 and 11.96 % for copper(II) and lead(II) ions, respectively (Fig. 7a). It may due to the evolution of a motive force of concentration gradient as the initial concentration [2,12].

Isotherm models: The equilibrium data of adsorption are tested with Langmuir, Freundlich and Temkin isotherm models. An isotherm is used to show the distribution of metal ions in two phases *i.e.* solid and liquid and the suitability of batch system for the adsorption phenomenon. Langmuir isotherm model is used to explain the monolayer adsorption of metal ions on the adsorbent which contains a definite number of functional or binding groups [15]. A linear equation of Langmuir isotherm model is given as below:

$$\frac{C_e}{Q_e} = \frac{1}{K_l X} + \frac{C_e}{K_l}$$

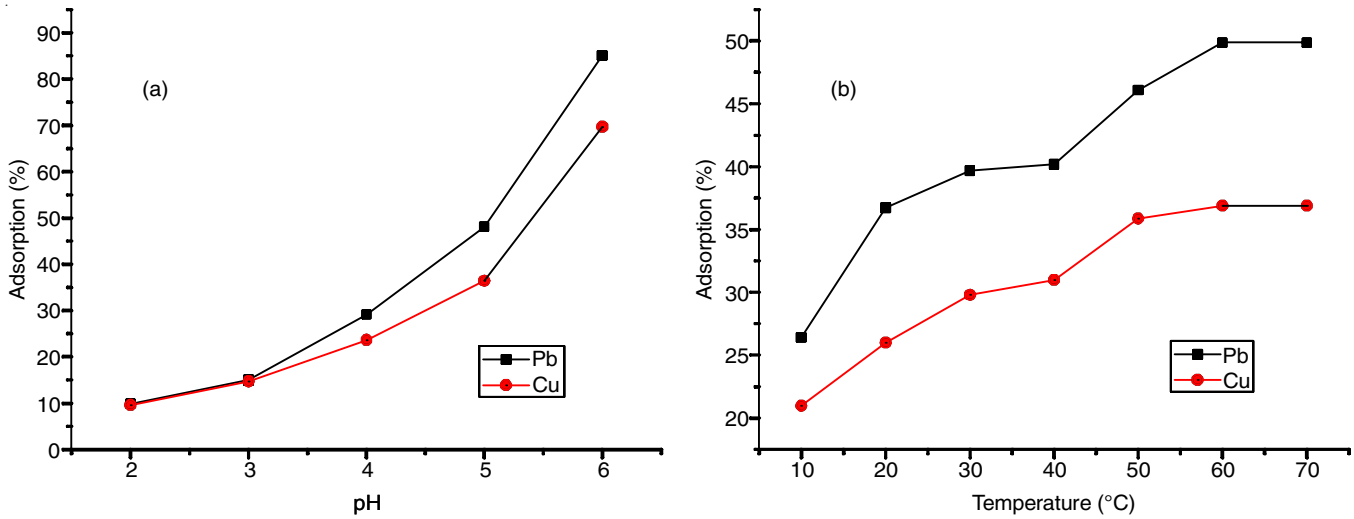

Fig. 6 (a) Effect of pH and (b) Effect of temperature on the removal of copper and lead

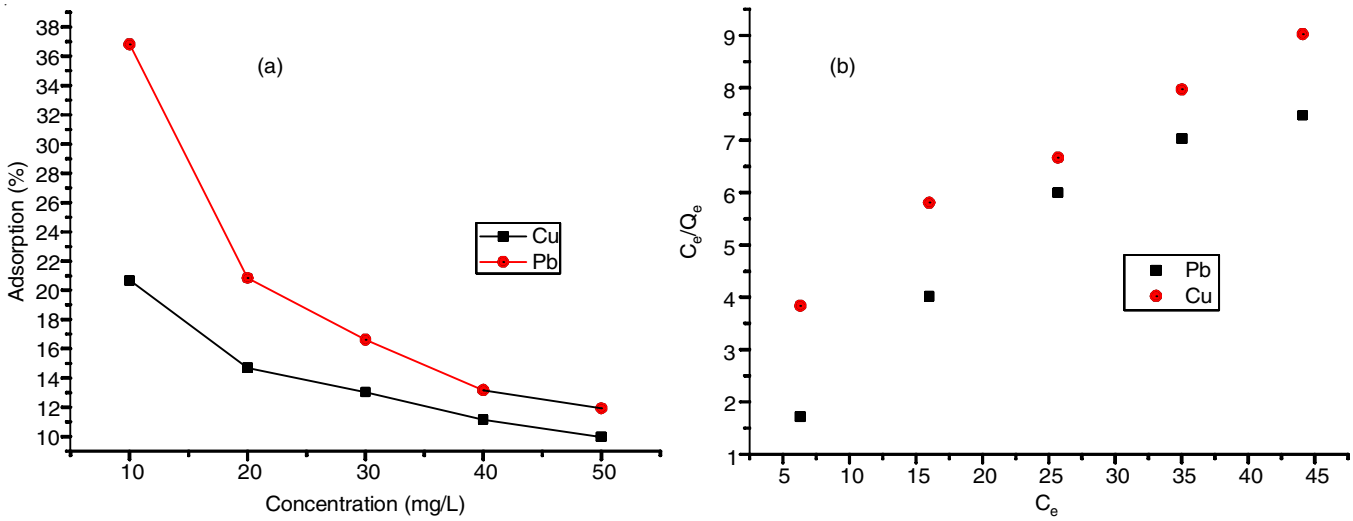

Fig. 7 (a) Effect of concentration and (b) Langmuir isotherm model

where, C_e and Q_e are the equilibrium concentration of metal ions in the solution after adsorption and amount of metal adsorbate per gram of adsorbent and K_1 and X are the adsorption capacity (mg/g) and adsorption equilibrium constant (L/mg). The values of K_1 and X have been calculated as 6.480 mg/g and 0.1167 L/mg for lead(II) and 7.535 mg/g and 0.0404 L/mg for copper(II) (Table-1). The values of correlation (R^2) are found 0.984 for copper(II) and 0.9383 for lead(II); it indicates that copper(II) follows Langmuir isotherm model more than lead(II). The characteristic feature of Langmuir isotherm model is a dimensionless parameter R_L which is mathematically defined as follows:

$$R_L = \frac{1}{1 + XC_o}$$

TABLE-1
VALUES OF ISOTHERMAL PARAMETERS

Isotherms	Metals	Parameters	Values
Langmuir	Pb	K_1 (mg/g)	6.480
		X (L/mg)	0.1167
		R^2	0.9383
	Cu	K_1 (mg/g)	7.535
		X (L/mg)	0.0404
		R^2	0.984
Freundlich	Pb	K_2 (mg/g)	2.312
		1/n	0.2187
		R^2	0.8034
	Cu	K_2 (mg/g)	1.155
		1/n	0.4599
		R^2	0.9928
Temkin	Pb	A (mg/g)	1.532
		B	0.9984
		R^2	0.7513
	Cu	A (mg/g)	0.8892
		B	1.500
		R^2	0.8892

Herein, C_o and X are the initial concentration of metal ions (mg/L) in the working solution and X is adsorption equilibrium constant (L/mg). The values of R_L are found $R_L < 1$ in all ranges of initial concentrations of copper(II) and lead(II) in the working solutions; it means the suitability of adsorption of metal ions on the nano-surface. The Freundlich isotherm model is related to the presence of different functional groups on the nano-surface and their involvement in the interactions with metal ions with different energies on the non-uniform nano-surface [2,12]. Mathematically, the linear Freundlich isotherm equation is given as below:

$$\log Q_e = \log K_2 + \frac{1}{n} \log C_e$$

where, Q_e, K_2, 1/n and C_e are the amount of metal adsorbate on the surface of adsorbent (mg/g), adsorption capacity, adsorption intensity and equilibrium metal ion concentration. The values of K_2 and 1/n have been calculated as 2.312 mg/g and 0.2187 for lead(II) and 1.155 mg/g and 0.4599 for copper(II) from the graph log Q_e *vs*. log C_e (figure not shown). The values of regression indicate that copper favours Freundlich isotherm model than lead(II) ions (Table-1). Temkin isotherm model is basically related to metal-metal interactions on the surface of adsorbent and a linear decrease of heat of adsorption with the coverage of adsorbed metal ions [2,12,13]. A linear form of Temkin model is represented as below:

$$Q_e = A + B \ln C_e$$

where, Q_e and C_e are the amount of metal adsorbed on the surface of 1 g adsorbent and metal ion concentrations (mg/L) in working solutions after adsorption; A and B are the adsorption capacity and Temkin constant. In this pattern, the adsorption capacity of adsorbent for lead(II) is more than copper(II) (Table-1).

Conclusion

Green synthetic method used to synthesize α-Fe_2O_3 nanoparticles is very efficient, low cost and ecofriendly method. The freshly prepared dried α-Fe_2O_3 nanoparticles have been found excellent nano-adsorbent to remove Cu(II) and Pb(II) ions from synthetically prepared wastewater. Maximum percentage adsorption was found at optimized conditions *i.e*. highest contact time, higher dosage of adsorbent, higher acidic pH and lower metal ion concentrations. The equilibrium data of adsorption of Cu(II) and Pb(II) ions on to the surface of α-Fe_2O_3 nanoparticles are best fitted to Langmuir isotherm model as compared to Freundlich and Temkin isotherm models.

CONFLICT OF INTEREST

The authors declare that there is no conflict of interests regarding the publication of this article.

REFERENCES

1. D. Mukherjee, S. Ghosh, S. Majumdar and K. Annapurna, *J. Environ. Chem. Eng.*, **4**, 639 (2016); https://doi.org/10.1016/j.jece.2015.12.010.
2. S. De Gisi, G. Lofrano, M. Grassi an M. Notarnicola, *Sustain. Mater. Technol.*, **9**, 10 (2016); https://doi.org/10.1016/j.susmat.2016.06.002.
3. A. Bhatnagar and A.K. Minocha, *Indian J. Chem. Technol.*, **13**, 203 (2006).
4. F. Fu and Q. Wang, *J. Environ. Manage.*, **92**, 407 (2011); https://doi.org/10.1016/j.jenvman.2010.11.011.
5. K.C. Kang, S.S. Kim, J.W. Choi and S.H. Kwon, *J. Ind. Eng. Chem.*, **14**, 131 (2008); https://doi.org/10.1016/j.jiec.2007.08.007.
6. A. Jusoh, L. Su Shiung, N. Ali and M.J.M.M. Noor, *Desalination*, **206**, 9 (2007); https://doi.org/10.1016/j.desal.2006.04.048.
7. Y. Li, F. Liu, B. Xia, Q. Du, P. Zhang, D. Wang, Z. Wang and Y. Xia, *J. Hazard. Mater.*, **177**, 876 (2010); https://doi.org/10.1016/j.jhazmat.2009.12.114.
8. M.I. Kandah and J.L. Meunier, *J. Hazard. Mater.*, **146**, 283 (2007); https://doi.org/10.1016/j.jhazmat.2006.12.019.
9. Y.H. Li, Z. Di, J. Ding, D. Wu, Z. Luan and Y. Zhu, *Water Res.*, **39**, 605 (2005); https://doi.org/10.1016/j.watres.2004.11.004.
10. A. Dabrowski, Z. Hubicki, P. Podkoœcielny and E. Robens, *Chemosphere*, **56**, 91 (2004); https://doi.org/10.1016/j.chemosphere.2004.03.006.
11. Z. Ai, Y. Cheng, L. Zhang and J. Qiu, *Environ. Sci. Technol.*, **42**, 6955 (2008); https://doi.org/10.1021/es800962m.
12. G.Z. Kyzas and M. Kostoglou, *Materials*, **7**, 333 (2014); https://doi.org/10.3390/ma7010333.
13. M. Sharma, R.K. Vyas and K. Singh, *Adsorption*, **19**, 161 (2013); https://doi.org/10.1007/s10450-012-9436-9.
14. A.S. Ayangbenro and O.O. Babalola, *Int. J. Environ. Res. Public Health*, **14**, 94 (2017); https://doi.org/10.3390/ijerph14010094.
15. M. Czikkely, E. Neubauer, I. Fekete, P. Ymeri and C. Fogarassy, Water, 10, 1377 (2018); https://doi.org/10.3390/w10101377.
16. M.J.K. Ahmed and M. Ahmaruzzaman, *J. Water Process Eng.*, **10**, 39 (2016); https://doi.org/10.1016/j.jwpe.2016.01.014.
17. Ihsanullah, A. Abbas, A.M. Al-Amer, T. Laoui, M.J. Al-Marri, M.S. Nasser, M. Khraisheh and M.A. Atiehef, *Sep. Purif. Technol.*, **157**, 141 (2016); https://doi.org/10.1016/j.seppur.2015.11.039.
18. N.S. Bhandari, N.C. Joshi, G.C. Shah and S. Kumar, *J. Indian Chem. Soc.*, **89**, 383 (2012).
19. A.S. Teja and P.Y. Koh, *Prog. Cryst. Growth Charact. Mater.*, **55**, 22 (2009); https://doi.org/10.1016/j.pcrysgrow.2008.08.003.
20. T. Neuberger, B. Schöpf, H. Hofmann, M. Hofmann and B. von Rechenberg, *J. Magn. Magn. Mater.*, **293**, 483 (2005); https://doi.org/10.1016/j.jmmm.2005.01.064.
21. I. García-Díaz, F.A. Lopez and F.J. Alguacil, *Metals*, **8**, 914 (2018); https://doi.org/10.3390/met8110914.
22. M. Ayyanar and P. Subash-Babu, *Asian Pac. J. Trop. Biomed.*, **2**, 240 (2012); https://doi.org/10.1016/S2221-1691(12)60050-1.
23. B. Turakhia, P. Turakhia and S. Shah, *South-Asian J. Multidiscipl. Stud.*, **5**, 132 (2017).
24. S.Z. Mohammadi, M. Khorasani-Motlagh, S. Jahani and M. Yousef, *Int. J. Nanosci. Nanotechnol.*, **8**, 87 (2012).
25. Y. Liu, J. Luan, C. Zhang, X. Ke and H. Zhang, *Environ. Sci. Pollut. Res.*, **26**, 10387 (2019); https://doi.org/10.1007/s11356-019-04459-w.
26. Q. Jin, C. Cui, H. Chen, J. Wu, J. Hu, X. Xing, J. Geng and Y. Wu, *Front. Environ. Sci. Eng.*, **13**, 16 (2019); https://doi.org/10.1007/s11783-019-1092-9.